

GA-A22398

**MEASUREMENTS OF DIVERTOR IMPURITY
CONCENTRATIONS ON DIII-D**

by

**R.D. WOOD, R.C. ISLER, S.L. ALLEN, M.E. FENSTERMACHER,
C.J. LASNIER, A.W. LEONARD, and W.P. WEST**

OCTOBER 1996

MEASUREMENTS OF DIVERTOR IMPURITY CONCENTRATIONS ON DIII-D

by

R.D. WOOD,[†] R.C. ISLER,[‡] S.L. ALLEN,[†] M.E. FENSTERMACHER,[†]
C.J. LASNIER,[†] A.W. LEONARD, and W.P. WEST

This is a preprint of a paper to be presented at the Twenty-Third European Conference on Controlled Fusion and Plasma Physics, June 24–28, 1996, Kiev, Ukraine, and to be published in the *Proceedings*.

[†]Lawrence Livermore National Laboratory

[‡]Oak Ridge National Laboratory

Work supported by
the U.S. Department of Energy
under Contract Nos. DE-AC03-89ER51114,
W-7405-ENG-48, and DE-AC05-96OR22464

GA PROJECT 3466
OCTOBER 1996

MEASUREMENTS OF DIVERTOR IMPURITY CONCENTRATIONS ON DIII-D*

R.D. Wood,[†] R.C. Isler,[‡] S.L. Allen,[†] M.E. Fenstermacher,[†] C.J. Lasnier,[†]
A.W. Leonard, and W.P. West

General Atomics, P.O. Box 85608, San Diego, California 92186-9784 U.S.A.

INTRODUCTION

One promising method of reducing the target plate heat load is to enhance the divertor radiation with deuterium and gaseous impurity injection.¹ On DIII-D, during discharges with heavy deuterium (D₂) gas injection, we have observed divertor peak heat flux reductions (~3-5x) at the target plate with a corresponding increase in radiative losses.² Reconstructed bolometer data show increased radiation in the outboard divertor extending from the X-point to the outer strikepoint (OSP).³ Furthermore, the electron pressure near the OSP decreases significantly, but only modest changes are observed farther out in the scrape off layer (SOL); i.e., these divertor plasmas are detached near the separatrix, but remain attached farther out in the SOL and are referred to as a Partially Detached Divertor (PDD).²

To characterize the constituents of the radiation in a PDD, emissions in the 100–1100 Å spectral region are measured with an absolutely calibrated SPRED⁴ spectrograph. The spectrograph has a vertical view of the lower divertor along the same line of sight as the eight-channel Divertor Thomson Scattering (DTS) system.⁵ One channel of the bolometer array has a similar line of sight as the SPRED and provides a line-integrated measurement of the total radiated power. The extent of the radiation zones of selected visible lines along the line of sight of the SPRED are determined from a tangentially-viewing TV camera⁶ with filters. This diagnostic set enables us to evaluate the power radiated from individual ions and to determine impurity densities in the divertor region.

During PDD operations, the divertor plasma was swept so that the field of view of the vertically viewing diagnostics (R=1.48 m) sampled the divertor region from the X-point to outside the OSP. Figure 1 shows a time trace of discharge parameters with D₂ puffing and a sweep of the divertor plasma. At 2500 ms D₂ gas is puffed into the vessel at the midplane, and increases in the core electron density and total radiated power are observed. The PDD begins to form at 3100 ms and from visible TV data (not shown) the carbon emissions shift from the inner scrape off layer near the X-point to a distributed region from the X-point to partially down the outer leg. The divertor plasma is slowly swept inward from 3200 ms to 4300 ms. During the sweep an abrupt increase in CIV emissions occur when the highly radiating zone enters the SPRED line-of-sight (3600 ms). As the divertor plasma is swept inward, CIV emissions decrease while the Ly-β emissions increase showing that carbon radiation dominates near the X-point and deuterium radiation dominates near the OSP.

DETERMINING ION DENSITIES AND TOTAL RADIATED POWER FROM SPECTROSCOPY

At divertor-relevant electron densities (n_e) and temperatures (T_e) on DIII-D, the bulk of the radiated power comes from the 400–1600 Å spectral region. In principle, the total radiated power can be determined by summing the absolute intensities from all significant transitions. However, some of the strong lines of deuterium (Ly-α, 1216 Å) and carbon (CIII, 1175 Å and CIV, 1550 Å) are outside the spectral region of the divertor SPRED instrument. For deuterium, the measured intensity of the Ly-β (1025 Å) transition is used to

*Work supported by the U.S. Department of Energy under Contract Nos. DE-AC03-89ER51114, W-7405-ENG-48, and DE-AC05-96OR22464.

[†]Lawrence Livermore National Laboratory.

[‡]Oak Ridge National Laboratory.

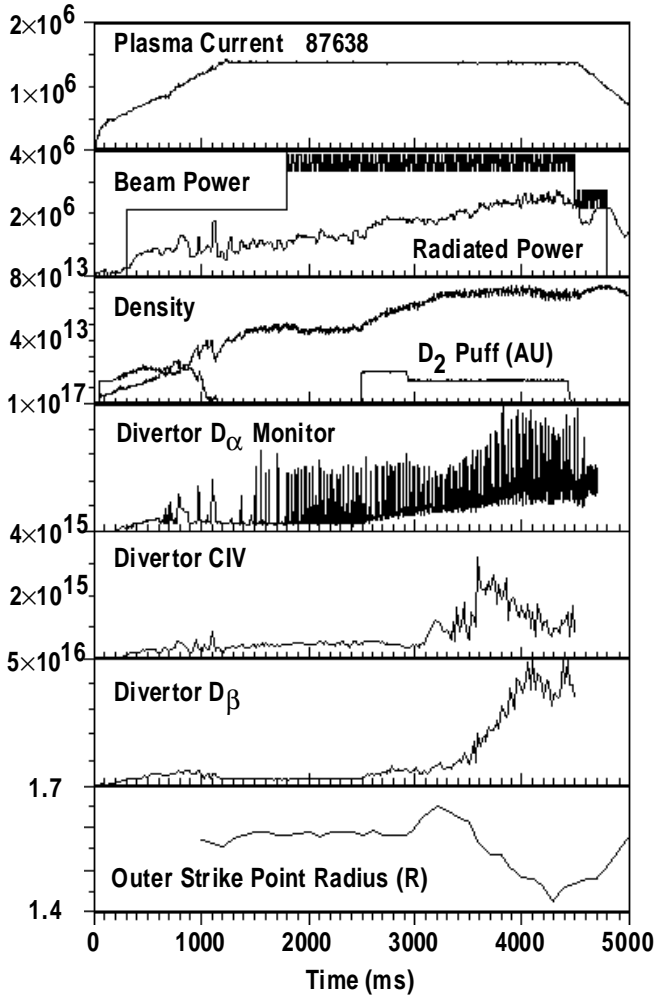


Fig. 1. Time traces of selected experimental parameters for a discharge with partially detached divertor and a sweep of the divertor plasma. At 2500 ms D₂ gas is puffed near the vessel midplane, and increases in the core n_e and total radiated power are observed. The PDD begins to form at 3100 ms and the divertor plasma is slowly swept inward from 3200 ms to 4300 ms. During the sweep an abrupt increase in CIV emissions occur when the highly radiating zone enters the SPRED line-of-sight (3600 ms). As the divertor plasma is swept inward, CIV emissions decrease while the Ly- β emissions increase.

The transport coefficients are adjusted until the calculated and measured line ratios are in good agreement. The total radiative losses are then compared to obtain correction factors for using the measured line ratios mentioned above. The transport code is used as a tool to predict line-of-sight profiles from the measured emissions and is not intended to model impurity transport in the divertor. In general, the spectroscopic determinations of power losses agree well with those from bolometry; during beam heated discharges, differences in the two results are less than 25%.⁸

CHARACTERIZATION OF INTRINSIC EMISSIONS

The effective electron temperatures from line ratios are found to vary little during a discharge, which indicates that a given ion tends to exist over a rather limited temperature range. Using this fact, the vertical

predict the Ly- α (1216 Å) contribution and to obtain the total deuterium radiated power using the Johnson and Hinnov⁷ results. For carbon it is necessary to employ collisional-radiative modeling to evaluate the total radiated power from measured transitions of ions. The effective T_e at the site of each ion is first determined from a spectral line ratio; the emitted power is then deduced from the emission of a single line using the inferred T_e .⁸ The effective T_e , derived from line ratios measured along the line of sight of the SPRED spectrograph, represents an average T_e over the radiating volume. This analysis is also used to provide line-integrated ion densities.

Over the temperature and density range of interest (2–20 eV, 1.0×10^{20}), the carbon radiation is due principally to emission by CIV at 1550 Å; the total contributions from CII and CIII are small (~20%). Determination of CIV power loss is complicated by the fact the measured line emission used to predict the total radiation is sensitive to both n_e and T_e ; transitions with a change in the principal quantum number ($\Delta n \neq 0$ transition) are generally sensitive to n_e and T_e . Furthermore, the temperature at which the measured CIV lines radiate is slightly higher than for the strong $\Delta n = 0$ transitions (CIV 1550 Å). As a result, the effective T_e , calculated from the measured line ratios is slightly elevated, which results in an underestimate of the total CIV radiated power. Thus, a simple one-dimensional transport code (STRAHL⁹) along with DTS measured n_e and T_e are used to predict the measured line ratios.

locations of the carbon ions and the n_e at these locations are established by correlating the effective electron temperatures with spatially resolved DTS data. The vertical location of the radiation zone determined from inversions of two-dimensional bolometer and visible TV data are in good agreement with those established from line radiation measured with the SPRED. For example, in PDD operation the CIII and CIV radiation is located in a region near the X-point.

A representative two-dimensional distribution of the radiated power density, and the carbon and deuterium fractional power during the OSP sweep is shown in Fig. 2. When the PDD forms, the carbon radiation zone at the X-point is in the field of view of the SPRED spectrograph and the bulk of the radiation comes from CIV. As the OSP is swept inward, the radiated power from deuterium increases until it dominates when the OSP is near the spectrograph line of sight. The carbon power fraction from the X-point along the outer leg of the divertor is ~80% of the total with the balance coming from deuterium. Near the OSP the deuterium power fraction is 60% of the total. These power fractions are similar to those reported on JT-60U where carbon has been reported as the major contributor to divertor radiation losses;¹⁰ the plasma facing surfaces of both DIII-D and JT-60U are constructed with carbon materials.

The carbon ion concentrations during the OSP sweep are also determined. They are obtained from the line-integrated ion densities by employing the images from the tangentially viewing TV camera equipped with a CIII filter to determine the extent of the radiation zone. During the sweep of the divertor plasma shown in Fig. 2, the estimated carbon concentrations range from 1% to 2% of the electron density.

CONCLUSIONS

Carbon emissions in the DIII-D divertor during partial detachment have been measured, and the deduced radiated power and the temporal behavior of the impurity emissions from spectroscopy are in good agreement with bolometer measurements. Effective electron temperatures from line ratios for CIV (9–11 eV) and CIII (6–8 eV) are correlated with DTS measured electron temperatures to determine the spatial location of the carbon radiation zone. During PDD operation, the bulk of the divertor radiation is emitted from CIV near the X-point while deuterium radiation is strongest near the outer strikepoint. The carbon ion concentrations are in the range of 1%–4% of the electron density.

REFERENCES

- ¹S.L. Allen, *et al.*, J. Nucl. Mater., **220–222**, (1995) 336.
- ²T.W. Petrie, *et al.*, J. Nucl. Mater., **196–198**, (1992) 848.
- ³A.W. Leonard, *et al.*, 22nd European Conf. on Controlled Fusion and Plasma Physics, Bournemouth, United Kingdom, Vol. 19C, Part III (1995) 105.
- ⁴R.J. Fonk, A.T. Ramsey, and R.V. Yelle, Appl. Optics **21**, 2115 (1982).
- ⁵S.L. Allen, *et al.*, “First Measurements of Electron Temperature and Density with Divertor Thomson Scattering in Radiative Divertor Discharges on DIII-D,” Proc. of 12th Conf. Plasma Surface Interactions, St. Raphael, France 1996.
- ⁶M.E. Fenstermacher, *et al.*, “A Tangentially Viewing Visible TV System for the DIII-D Divertor,” Proc. of 11th High Temperature Plasma Diagnostics, Monterey, California, to be published in Rev. Sci Instrum. 1996.
- ⁷L.C. Johnson and E. Hinnov, J. Quant. Spectros. Rad. Transfer **13**, 333 (1973).
- ⁸R.C. Isler, *et al.*, “Spectroscopic Characterization of the DIII-D Divertor,” to be submitted to Physics of Plasmas, 1996.
- ⁹K. Behringer, JET Report JET-R(87)08, 1987.
- ¹⁰H. Kubo, *et al.*, Nucl. Fusion **33**, 1427 (1993).

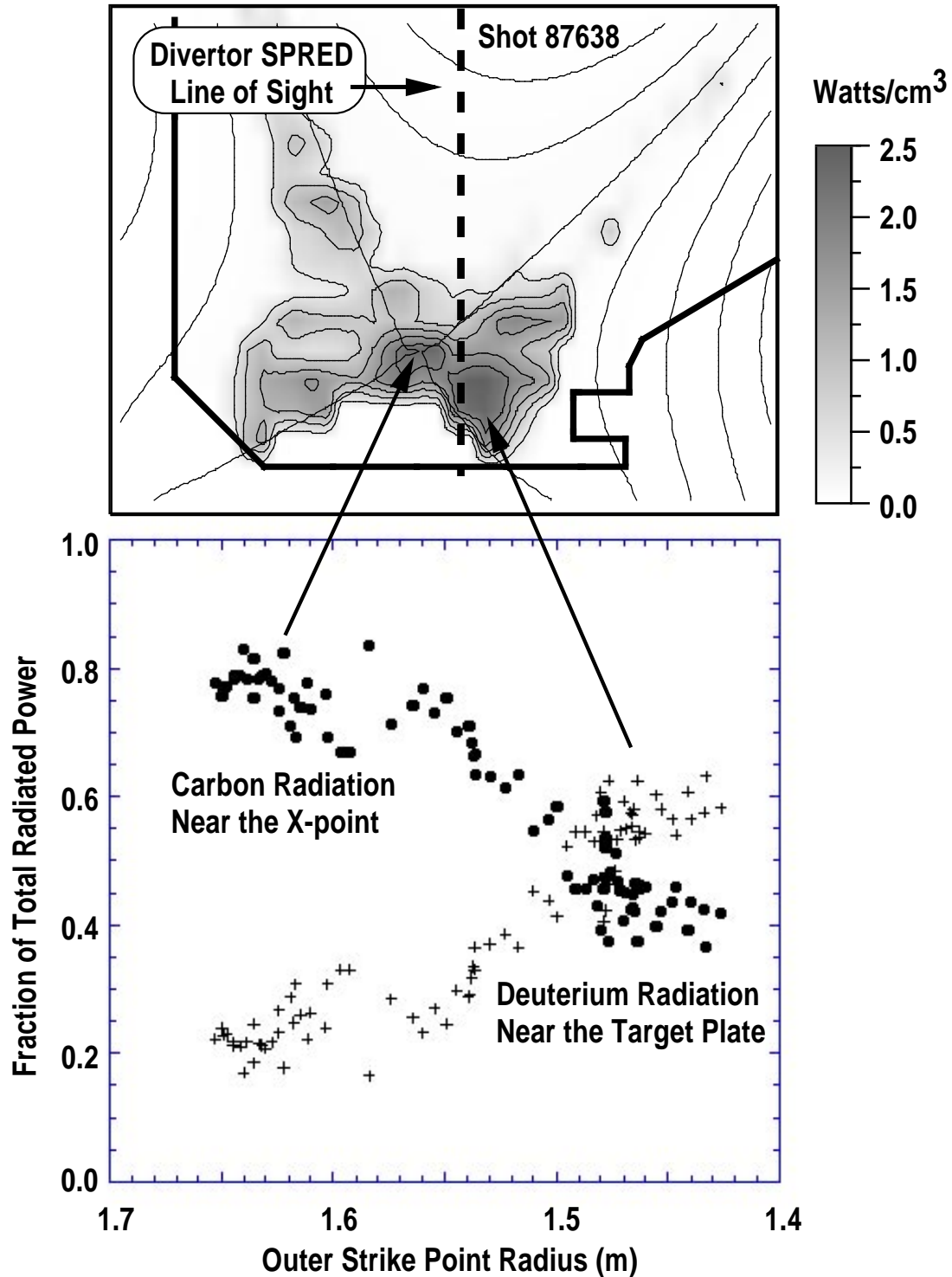


Fig. 2. (Top) Two-dimensional radiated power density distribution from reconstructed bolometer data obtained at 3800 ms during a sweep of the divertor plasma. (Bottom) Reconstructed spatial variation of SPRED data showing carbon (circles) and deuterium (+s) power fraction as a function of outer strike point location. The divertor plasma was swept across the divertor floor such that the axis of the vertically viewing diagnostics intercept the divertor region from the X-point, then along the outer leg to the outer strikepoint. Near the X-point most of the radiation is emitted from carbon (80%) with the balance from deuterium; near the target plate deuterium radiation dominates (60%).